

Thermoelectric Properties of Bi₂Te₃ / Sb₂Te₃ Thin Films

L.M.Goncalves^{1a}, C.Couto^{1b}, P.Alpuim^{2c}, D.M.Rowe^{3d}, J.H.Correia^{1e}

¹ University of Minho, Department of Electronics, Portugal

² University of Minho, Department of Physics, Portugal

³ Cardiff University, NEDO, United Kingdom

^algoncalves@dei.uminho.pt, ^bccouto@dei.uminho.pt, ^cpalpuim@fisica.uminho.pt,

^dRoweDM1@cardiff.ac.uk, ^ejhc@dei.uminho.pt

Keywords: thermoelectric, thin film, Peltier, micro-cooler,

Abstract. The deposition and characterization of n-type Bi₂Te₃ and p-type Sb₂Te₃ semiconductor films are reported. The films were deposited by thermal co-evaporation on a 25 μm thick polyimide (kapton) substrate. The co-evaporation method is inexpensive, simple, and reliable, when compared to other techniques that need longer time periods to prepare the starting material or require more complicated and expensive deposition equipment. Seebeck coefficients of -189 μVK⁻¹ and +140 μVK⁻¹ and electrical resistivities of 7.7 μΩm and 15.1 μΩm were measured at room temperature on n-type and p-type films, respectively. These values are better than those reported for films deposited by co-sputtering or electrochemical deposition, and are close to those reported for films deposited by metal-organic chemical vapour deposition or flash evaporation. Because of their high figures of merit, these films will be used for the fabrication of a micro-Peltier element, useful in temperature control and laser-cooling for telecommunications.

Introduction

In recent years local cooling and electric power generation using microdevices that work based on the Peltier and Seebeck effects is a topic of growing interest. Thermoelectric cooling based on Peltier effect has the advantages of not using any moving mechanical parts, being environmental friendly, allowing integration with microelectronic circuits and being easy to control. The Seebeck effect is used in electrical generators, converting thermal to electric energy.

In terms of their thermoelectric properties thermal devices are characterized by the parameter figure of merit (Z):

$$Z = \frac{\alpha^2}{\rho\lambda} \quad (1)$$

where α is the Seebeck coefficient, ρ the electrical resistivity, λ the thermal conductivity [1]. Often, the equivalent parameter 'figure of merit' = ZT, where T is the temperature in K, is used instead of Z.

Although there is no physical limit for the value of Z, thermoelectric materials did not exceed ZT ~ 1 for almost 50 years. Nevertheless, in the last few years a significant improvement in material properties was reported. Venkatasubramanian et al. [2] reports a figure of merit of ZT = 2.4 in ultra-thin layers of two alternating semiconductors. Many research groups are looking for new materials, with better figures of merit, and compatible with solid-state electronics. Tellurium alloys are well-established low-temperature thermoelectric materials that are widely employed in thermoelectric generators and coolers [1].

The conventional processes to produce these materials are not applicable to microelectronic devices, mainly because of the reduced dimensions of the devices (see for example [1]). Thin film planar technology is adequate for this task. Different deposition processes have been reported for deposition of Bi-Sb-Te thin films. Thermal co-evaporation [3], co-sputtering [4], electrochemical

deposition [5], metal-organic chemical vapour deposition [6] or flash evaporation [7] are some examples.

Two different approaches can be used to on-chip integration of thermoelectric coolers: transversal (cross-plane) and lateral (in-plane), depending on the direction in which energy is removed, relative to the surface of the device. In this work, lateral cooling is addressed, due to its easier fabrication process and compliance with planar technology (Fig. 1 and Fig. 2).

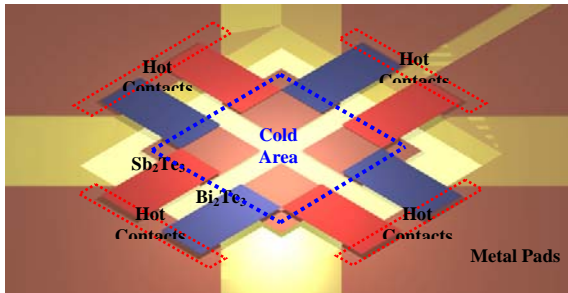


Fig. 1: In-plane (lateral) Peltier cooler

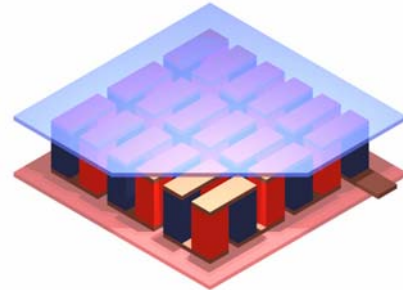


Fig. 2: Cross-plane (transversal) Peltier cooler

Thin Film Fabrication

Tentative deposition of Bi_2Te_3 and Sb_2Te_3 films by direct evaporation of the bulk materials proved to be impossible due to the large differences in vapour pressure of bismuth (or antimony) and tellurium, resulting in a compositional gradient along the film thickness. This result confirmed similar reports in the literature [8].

Co-evaporation of Bi and Te or Sb and Te was used to deposit n-type and p-type films, respectively, in a high-vacuum chamber with base pressure $< 5 \times 10^{-6}$ Torr. Two crystal oscillators with thickness monitors were used to monitor the deposition rate of Bi/Sb and Te. Each deposition rate was maintained at a fixed value, by controlling the power applied to each molybdenum evaporation boat. A computed PID controller was connected to the thickness monitors and to the deposition system and designed to real-time compute the power necessary to apply to the evaporation boats in order to achieve constant evaporation rates. Large molybdenum boats (baffled boxes) were used, in order to ease stable evaporation rates. Substrates were heated in the range 240 °C to 300 °C for bismuth telluride deposition and 200 °C to 260 °C for antimony telluride deposition. Fig. 3 shows a 580nm thick Bi_2Te_3 film deposited on a glass substrate and Table 1 summarizes the deposition parameters used for fabrication of n-type and p-type films.

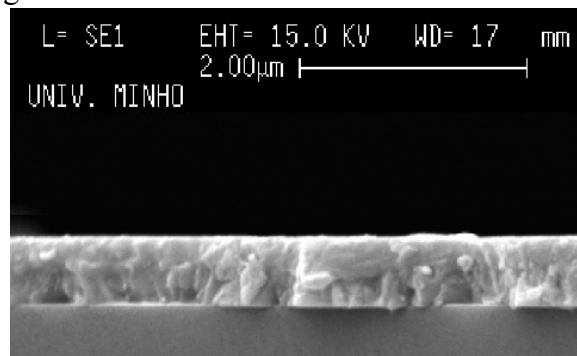


Fig. 3: A SEM photo of a homogeneous n-type 580 nm-thick Bi_2Te_3 film deposited onto a glass substrate.

Table 1. Parameters adjusted on film growing

Film	Substrate Temperature	Evaporation rate (Bi or Sb)	Evaporation rate (Te)
Bi_2Te_3	270 °C	1 A°/sec	2.2 A°/sec
Sb_2Te_3	230 °C	1 A°/sec	2.2 A°/sec

Both glass and polyimide (kapton) were used as substrates, with good adhesion of film to substrate. However, for the thermoelectric cooler circuit, 25 μm -thick kapton films were chosen as substrate because of their lower thermal conductivity ($0.12 \text{ Wm}^{-1}\text{K}^{-1}$) and their value of thermal expansion coefficient ($12 \times 10^{-6} \text{ K}^{-1}$) which closely matches the thermal expansion coefficient of the semiconductor films, thus reducing residual stress and increasing adhesion. Flexible substrates add uncommon mechanical properties to the composite film-substrate thus enabling their integration in many novel types of devices.

Material Characterization

Table 2 shows results from energy-dispersive X-ray (EDX) spectroscopic measurements for the best n-type and p-type films. Te and Bi (Sb) content shows that the composition of both types of films is close to stoichiometry.

Table 2. Stoichiometry of films measured by EDX

<i>Film</i>	<i>Te</i>	<i>Bi or Sb</i>
Bi ₂ Te ₃	60.17%	39.83%
Sb ₂ Te ₃	58.51%	41.49%

X-ray diffraction analysis (fig. 4 and fig. 5) reveals the polycrystalline structure of Bi₂Te₃ and Sb₂Te₃ materials. The peaks agree with the powder diffraction spectrum of polycrystalline Bi₂Te₃ and Sb₂Te₃.

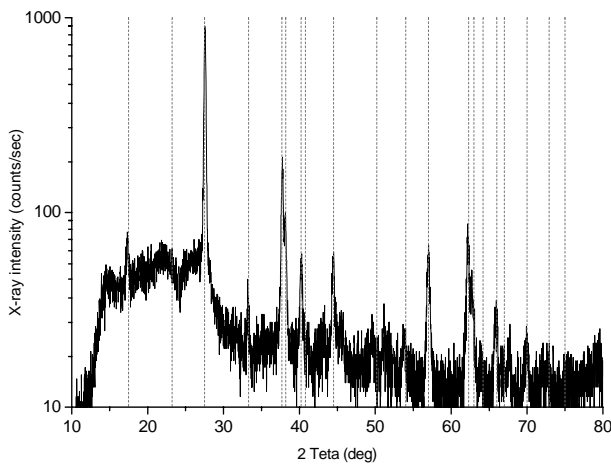


Fig. 4. XRD analysis of an n-type Bi₂Te₃ thin film. The peaks agree with the powder diffraction spectrum for Bi₂Te₃ (dashed lines).

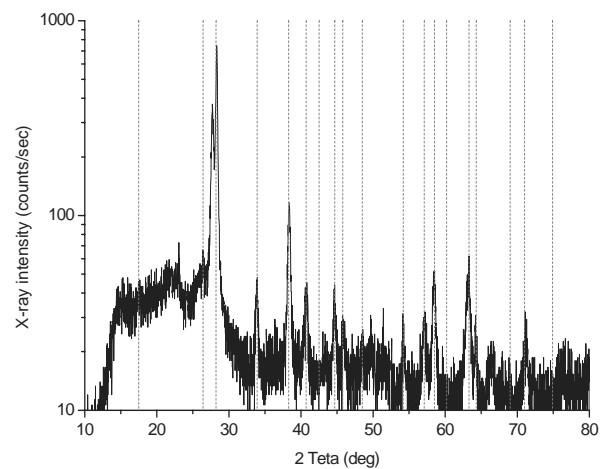


Fig. 5. XRD analysis of a p-type Sb₂Te₃ thin film. The peaks agree with the powder diffraction spectrum for Sb₂Te₃ (dashed lines).

Seebeck coefficient and electrical resistivity were also measured. Room temperature in-plane resistance was measured using the conventional four probe van der Pauw method. The Seebeck coefficient was measured by connecting one side of the film to a body at constant temperature (a heated metal block) and the other side to a heat sink at room temperature. Table 3 shows the results of these measurements and the respective figures of merit at 300 K (thermal conductivity of 1.5 Wm⁻¹K⁻¹ was assumed for calculations).

Table 3. Thermoelectric properties of co-evaporated films in the present work

<i>Film</i>	<i>Seebeck</i> [$\mu\text{V}/^\circ\text{C}$]	<i>Resistivity</i> [$\mu\Omega\text{m}$]	<i>Figure of merit (ZT)</i>
Bi ₂ Te ₃	-189	7.7	0.93
Sb ₂ Te ₃	140	15.1	0.26

The calculated values for the figure of merit are higher than those reported for films deposited by co-sputtering and by electrochemical deposition, and are close to those reported for films deposited by metal-organic chemical vapour deposition or by flash evaporation (Table 4). Performance of Bi₂Te₃ films is higher than that reported for bulk material whereas Sb₂Te₃ films perform slightly poorly than in bulk. (Thermal conductivity of 1.5 Wm⁻¹K⁻¹ was assumed to calculate figure of merit in Table 4.)

Table 4. Values of thermoelectric properties of state-of-the-art materials taken from literature.

<i>Film</i>	<i>Fabrication Method</i>	<i>Seebeck</i> [$\mu\text{V}/^\circ\text{C}$]	<i>Resistivity</i> [$\mu\Omega\text{m}$]	<i>Figure of merit (ZT)</i>
Bi ₂ Te ₃	Co-Sput. [4]	-160	16.3	0.31
Bi ₂ Te ₃	MOCVD [6]	-210	9.0	0.98
Bi ₂ Te ₃	Co-Evap. [3]	-228	13	0.80
Bi ₂ Te ₃	ECD. [5]	-60	10	0.07
Bi ₂ Te ₃ *	Flash [7]	-200	15	0.53
Sb ₂ Te ₃	MOCVD [6]	110	3.5	0.69
Sb ₂ Te ₃	Co-Evap. [3]	171	10.4	0.56

Device Simulation

A Peltier cooler, based on the n-type and p-type materials described above, is under construction using a kapton substrate. Both SPICE simulation and finite element analysis (FEM), considering radiation and convection losses, show the possibility to obtain $\sim 18^\circ\text{C}$ cooling between hot and cold sides of the device. Each p-n thermoelectric pair of the Peltier cooler can be modelled [9] by Eq. 2.

$$\Delta T = \frac{1}{K_e} (\alpha_p - \alpha_n) T_c I - \frac{1}{2} R_e I^2 - q_L \quad (2)$$

ΔT is the maximum temperature difference achieved by the cooler, α_p and α_n are the Seebeck coefficients of the materials, T_c is the cold side temperature, I is the current injected into the device

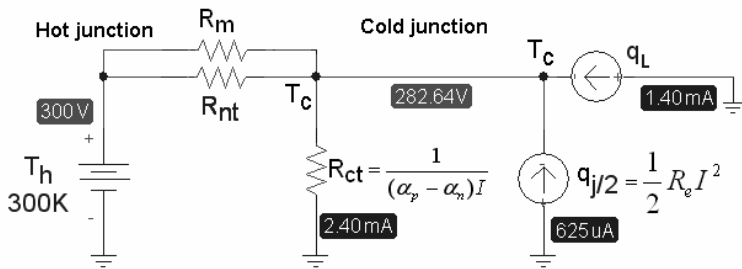


Fig. 6. Schematic model and simulation results of a Peltier cooler.

and q_L is the sum of all convective and radiative thermal loads applied. R_e and K_e are the equivalent electrical resistance and thermal conductance, respectively, of n and p elements, including the effect of substrate and contact resistances. Equation 2 is only valid if the hot side of the cooler is connected to a highly thermally conductive material and to a heat sink, capable of keeping the hot side temperature, T_h , at 300 K. The thermal circuit of the cooler can be modelled with an electrical SPICE simulator, using schematic model shown in Fig. 6. R_m (148.5 K Ω) and R_{nt} (66.66 K Ω) represent membrane and thermoelectric element thermal resistances, respectively. R_{ct} represents the heat removed by Peltier effect, q_L represents convection and radiation loss and $q_{j/2}$ is Joule heating at the cold side. The voltages on Fig. 6 represent the temperatures and the currents the thermal fluxes.

For FEM simulations, the thermal energy absorbed or released by Peltier effect at the junctions was calculated using $q = (\alpha_p - \alpha_n)IT$ and was applied as an external load (positive for the hot junction and negative for the cold junction). The RI^2 heating was also calculated and applied to the relevant volumes. Radiative and convective losses were calculated using, respectively, Stefan-Boltzmann's law and an approximated global coefficient [10]. Calculated radiative and convective losses were 7 $\text{Wm}^{-2}\text{K}^{-1}$ and 5 $\text{Wm}^{-2}\text{K}^{-1}$, respectively. The FEM simulation results (Fig. 7) map the temperature of the device. Convergence ($<0.1^\circ\text{C}$ error) was achieved after ~ 5 iterations starting with an arbitrary value of T_c , chosen from a plausible interval of temperature, while keeping $T_h = 300\text{ K}$. After each iteration, the estimated value of the energy absorbed at the cold junction of the Peltier device, for a given current ($I = 25\text{ mA}$) was recalculated until the condition $\Delta T = T_h - T_c$ is fulfilled.

Seebeck coefficients of $-190\ \mu\text{VK}^{-1}$ (n-type), $150\ \mu\text{VK}^{-1}$ (p-type), electrical resistivity of $10\ \mu\Omega\text{m}$ and thermal conductivity of $1.5\ \text{Wm}^{-1}\text{K}^{-1}$ were used in simulations. Each thermoelectric leg has dimensions of 2 mm length by 1 mm width by $10\ \mu\text{m}$ height, and the device stands on a $25\ \mu\text{m}$ -thick kapton substrate. The optimal current in the device [9] for this problem was calculated and used in the simulations ($I = 25\text{ mA}$).

Electrical contact resistance of $10^{-9}\ \Omega\text{m}^2$ was assumed for simulations. The thermal contact resistance was not included. Considering the dimensions of the devices, the contact resistances could be neglected compared with electrical and thermal resistances, as demonstrated in the literature [9].

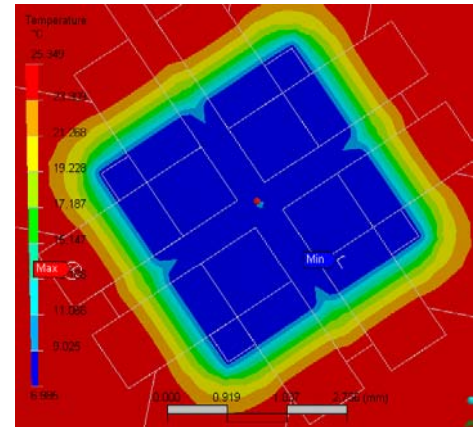


Fig. 7. FEM analysis shows the possibility of achieving 18°C cooling between the hot side and the cold side of the device, when the optimal current of 25mA is applied, and radiation and convection losses considered.

Conclusions

State-of-the-art Bi_2Te_3 and Sb_2Te_3 materials were deposited in the form of thin films by co-evaporation with film thickness ranging from 500 nm to 2 μm . Co-evaporation is a relatively simple and inexpensive method that allows deposition of good thermoelectric material, with large figures of merit. The effect of the evaporation rate and substrate temperature in thermoelectric properties of the films was studied, and the deposition process was optimized.

Calculations and FEM simulations showed the possibility of achieving more than 18 °C cooling in a Peltier device fabricated on a kapton polyimide substrate. Kapton's low thermal conductivity, good substrate adhesion and mechanical flexibility make it a good choice for the fabrication of lateral Peltier devices. Future work will include thin silicon nitride free-standing bridges fabricated by back-side wet etching. The use of silicon opens the possibility to integrate electronics, sensors and the cooler itself on the same silicon chip.

References

- [1] D.M. Rowe, "CRC Handbook of Thermoelectrics," CRC Press, (1995).
- [2] R. Venkatasubramanian, E. Siivola, T. Colpitts, and B. O'Quinn, "Thin-film thermoelectric devices with high room-temperature figures of merit," *Nature*, vol. 413, 6856, 597, (2001).
- [3] Helin Zou, D.M. Rowe, S.G.K. Williams, "Peltier effect in a co-evaporated $\text{Sb}_2\text{Te}_3(\text{P})$ - $\text{Bi}_2\text{Te}_3(\text{N})$ thin film thermocouple," *Thin Solid Films*, 408, 270, (2002)
- [4] Harald Böttner, Joachim Nurnus, Alexander Gavrikov, Gerd Kühner, Martin Jägle, Christa Künzel, Dietmar Eberhard, Gerd Plescher, Axel Schubert, and Karl-Heinz Schlereth, "New Thermoelectric Components Using Microsystem Technologies," *Journal of Microelectromechanical Systems*, 3, 414, (2004)
- [5] J.R. Lim, G.J. Snyder, C.K. Huang, J.A. Herman, MA. Ryanand, J.P. Fleurial, "Thermoelectric Microdevice Fabrication Process and Evaluation at the Jet Propulsion Laboratory," ICT2002
- [6] A. Giani, A. Boulouz, F. Pascal-Delannoy, A. Foucaran, E. Charles, A. Boyer, "Growth of Bi_2Te_3 and Sb_2Te_3 thin films by MOCVD," *Materials Science and Engineering*, B64, 19–24, (1999)
- [7] A. Foucaran, "Flash evaporated layers of $(\text{Bi}_2\text{Te}_3\text{--}\text{Bi}_2\text{Se}_3)(\text{N})$ and $(\text{Bi}_2\text{Te}_3\text{--}\text{Sb}_2\text{Te}_3)(\text{P})$," *Materials Science and Engineering*, B52, 154–161, (1998)
- [8] Luciana W. da Silva and Massoud Kaviani, "Miniaturized Thermoelectric Cooler," IMECE'02
- [9] Gao Min, D.M. Rowe, "Cooling performance of integrated thermoelectric Microcooler," *Solid-State Electronics*, 43, 923-929, (1999)
- [10] J.P. Holman, "Heat Transfer," Mc Graw Hill, (1989).